

# Error Resilience for Compressed Sensing with Multiple-Channel Transmission

Hsiang-Cheh Huang

Department of Electrical Engineering  
National University of Kaohsiung  
700 University Road, Kaohsiung 811, Taiwan, R.O.C.  
hch.nuk@gmail.com

Feng-Cheng Chang\*

Department of Innovative Information and Technology  
Tamkang University  
180 Linwei Road, Jiaosi, Ilan 262, Taiwan, R.O.C.  
\*Corresponding author.  
135170@mail.tku.edu.tw

Received November, 2014; revised April, 2015

---

**ABSTRACT.** *Compressed sensing, a newly developed scheme in data compression, has attracted much attention in researches due to its new concepts and superior performances over conventional techniques. Besides looking for compression performances, it would be practical to aim at data transmission of compressed information, and few papers in this field can be found in literature. For the transmission of compressed information, because it is vulnerable to channel errors, error resilience for compressed information has long been a practical topic for researches and applications. With compressed sensing, very few amounts of coefficients are capable of reconstructing the image with reasonable quality. In this paper, for the delivery of compressively sensed coefficients over independent and lossy channels, reconstructed image with reasonable quality over a variety of lossy rates can be obtained. Simulation results have pointed out that with the proposed algorithm, the applicability and superiority in performances can be acquired over conventional algorithm in compressed sensing.*

**Keywords:** Compressed sensing, Error resilience, Reconstruction.

---

**1. Introduction.** Data compression has long been an important topic in the field of signal processing. With the widely use of smartphone cameras or tablets, vast amounts of multimedia contents, mostly images, have accumulated drastically. Thus, how to efficiently perform data compression on the multimedia contents would be in urgent needs. There have been successful and popular standards for image compression, including the use of transform coding [1], like discrete cosine transform (DCT) for JPEG and discrete wavelet transform (DWT) for JPEG2000, and vector quantization (VQ) [2], for the compression of still images. With the evolution of new techniques, advancements in data compression can also be expected, and compressed sensing technique presents new concepts and some novelties over its predecessors.

Compressed sensing [3, 4] is a newly developed branch in data compression researches in the last couple of years. It requires the sampling rate, which is far less than the Nyquist

rate, with the capability of reconstructing the original signal to be above some acceptable level. There is a website [5] that arranges topics in compressed sensing. Papers in this field aim mainly at theoretic derivations [6, 7], and optimization techniques can be included to solve compressed sensing as non-linear optimization problems [8]. From practical point of view, there are applications to extend compressed sensing to image compression [9, 10] or watermarking [11, 12]. There are few papers that aim at the transmission of compressed sensing signals [13], and this is the motivation to devise algorithm and conduct experiments in this paper.

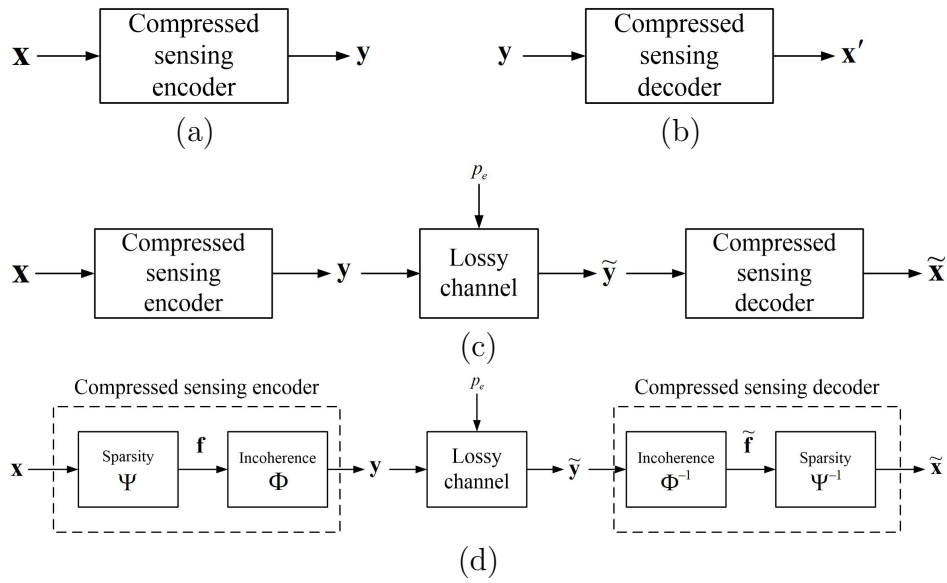


FIGURE 1. Basic structures and notations for compressed sensing. (a) Diagram of encoding part. (b) Diagram of decoding part. (c) Data transmission with compressed sensing. (d) Notations with sparsity and incoherence in compressed sensing.

Fig. 1 demonstrates the conventional approach in data compression. Here, we use digital images to play the roles of input and output data. In Fig. 1(a), at the encoder, let the input image be  $\mathbf{x}$ . After applying compression, compressed sensing as an instance, at the encoder, compressed signal  $\mathbf{y}$  can be obtained. The size of  $\mathbf{y}$  should be much fewer than that of  $\mathbf{x}$ . In Fig. 1(b), at the decoder, compressed signal  $\mathbf{y}$  is ready for decoding with the corresponding decompression technique at the decoder, again compressed sensing as an instance. After calculations with the decompression procedures, reconstructed image  $\mathbf{x}'$  can be acquired. We would expect that  $\mathbf{x}$  and  $\mathbf{x}'$  look as resemble as possible. From another perspective, the difference between  $\mathbf{x}$  and  $\mathbf{x}'$  should be as small as possible. We also note that the block of compressed sensing encoding in Fig. 1(a), and the one of compressed sensing decoding in Fig. 1(b), can be simultaneously replaced with other standards such as JPEG or JPEG2000 compression. It follows directly from conventional data compression, thus these techniques share the same concept as depicted in Fig. 1.

It would be more practical for the transmission of compressed signals over the lossy channel to the decoder, as depicted in Fig. 1(c). Corresponding to Fig. 1(a) and Fig. 1(b), let the input image be  $\mathbf{x}$  at the encoder. After performing compression at the encoder, compressed signal  $\mathbf{y}$  need to be transmitted to the decoder over the lossy channel. Due to the channel errors induced, with the probability of  $p_e$  during transmission, the reception of compressed signal  $\tilde{\mathbf{y}}$  may be different from its counterpart  $\mathbf{y}$ . Finally, at the decoder,  $\tilde{\mathbf{y}}$  need be decompressed to obtain the reconstructed image  $\tilde{\mathbf{x}}$ . We may expect

the quality degradation in  $\tilde{\mathbf{x}}$  to compare with  $\mathbf{x}'$ , and possible means to alleviate this phenomenon can be devised to make error resilient transmission possible. In this paper, besides the compression capabilities, we also aim at error resilient transmission over lossy channels. With the proposed scheme, effects caused by channel errors can be alleviated, and recovered image quality can be improved.

This paper is organized as follows. In Sec. 2, we briefly describe the fundamentals and mathematical representations of compressed sensing. In Sec. 3, we present the proposed method for error resilient transmission of compressed sensing signals over independent and lossy channels. Simulation results are demonstrated in Sec. 4, which point out the vulnerability of compressively sensed signals for the transmission over a single channel, and the alleviation of image quality degradation with our algorithm for multiple channel transmission. Finally, we address the conclusion of this paper in Sec. 5.

**2. Fundamental Descriptions and Notations of Compressed Sensing.** Compressed sensing aims at looking for new sampling scheme that goes against conventional sampling theorem, or the widely acquainted Nyquist-Shannon theorem. With compressed sensing, a much smaller rate than twice the maximal bandwidth can be achieved to meet perfect recovery of reconstruction.

In compressed sensing, it comprises the *sparsity* and the *incoherence* principles [14, 15], as depicted in Fig. 1(c). By following the notations in Figs. 1(a) and 1(b), we can easily observe Fig. 1(d) is the direct extension to Fig. 1(c). The two principles are described as follows.

- For the *sparsity* principle, it implies the information rate in data compression. In compressed sensing, it is expected to reach a much smaller sampling rate than conventional one required, and it can be represented with the proper basis  $\Psi$ ,  $\Psi \in C^{N \times N}$ , and  $C$  denotes the complex number in the  $N \times N$  matrix. More specifically,  $\Psi$  is the basis to reach sparsity with a  $k$ -sparse coefficient vector  $\mathbf{x}$ ,  $\mathbf{x} \in C^{N \times 1}$ , with the condition that

$$\mathbf{f} = \Psi \mathbf{x}. \quad (1)$$

Here,  $\mathbf{f} = [f_1, f_2, \dots, f_N]^T$  denotes the reconstruction corresponding to the original signal, and  $f_i$  denotes the coefficients of the  $i^{\text{th}}$  basis.

- For the *incoherence* principle, it extends the duality between time and frequency. The measurement basis  $\Phi$ ,  $\Phi \in C^{m \times N}$ , which acts like noiselet, is employed for sensing the signal  $\mathbf{f}$ , with the condition that

$$\mathbf{y} = \Phi \mathbf{f}. \quad (2)$$

Here,  $\mathbf{y}$  denotes the measurement vector, as depicted in Fig. 1(a). Because  $m$  implies the number of measurement coefficients, it should be much less than the image size  $N$ , or  $m \ll N$ . We note that Eq. (2) is an underdetermined system.

In Fig. 1(b), it is the reverse process to its counterparts in Fig. 1(a). Thus, we may reach the condition that [9]

$$\mathbf{x}' = \Psi^H (\Psi \Psi^H)^{-1} \mathbf{y}. \quad (3)$$

In Eq. (3), the superscript  $H$  denotes the Hermitian operation. Considering Eq. (1) and Eq. (2), by minimizing the  $l_1$ -norm of  $\mathbf{x}$ , i.e.,  $\min \|\mathbf{x}\|_1$ , subject to  $\Phi \Psi \mathbf{x} = \mathbf{y}$ , compressed sensing guarantees the perfect recovery with probability close to 1.0. Besides, because of looking for  $\min \|\mathbf{x}\|_0$ , or  $l_0$ -minimization is an NP-hard combinatorial problem, we look for  $l_1$ -minimization instead, and this follows the implementations in [9].

**3. Proposed Algorithm.** It is easily observed that sub-sampled images have high correlations with each other, and these correlations may help to recover the reconstructed image after transmission. For original image  $\mathbf{x}$  with the size of  $N = K \times L$  in Eq. (1),  $\mathbf{x} = x(i, j)$ ,  $1 \leq i \leq K$  and  $1 \leq j \leq L$ , the four sub-sampled images  $\mathbf{x}_1$ ,  $\mathbf{x}_2$ ,  $\mathbf{x}_3$ , and  $\mathbf{x}_4$ , can be represented by

$$\mathbf{x}_1 = x_1(i, j) = x(2i - 1, 2j - 1), \quad (4a)$$

$$\mathbf{x}_2 = x_2(i, j) = x(2i - 1, 2j), \quad (4b)$$

$$\mathbf{x}_3 = x_3(i, j) = x(2i, 2j - 1), \quad (4c)$$

$$\mathbf{x}_4 = x_4(i, j) = x(2i, 2j). \quad (4d)$$

Here,  $1 \leq i \leq \frac{K}{2}$  and  $1 \leq j \leq \frac{L}{2}$ . By use of the correlations, we may expect to obtain enhanced quality in reconstructed image for error-resilience transmission. The overall structure can be depicted in Fig. 2.

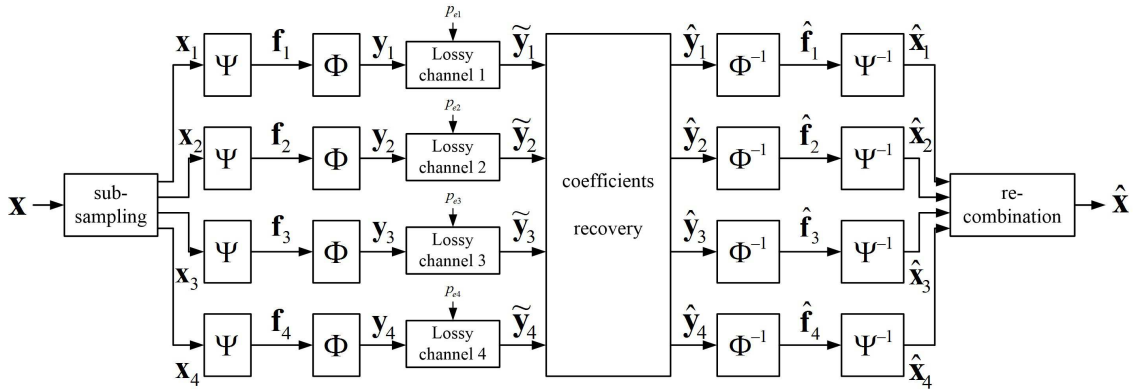


FIGURE 2. Multiple-channel transmission and recovery for compressed sensing.

From the experiences in data compression [1], due to the fact that compressed multimedia contents are vulnerable to channel errors, error-controlled transmission would be required. During delivery from the encoder to the decoder, we employ the concept of multi-channel transmission to alleviate the degradation of reconstructed image quality.

In Fig. 2, the four sub-sampled images  $\mathbf{x}_1$ ,  $\mathbf{x}_2$ ,  $\mathbf{x}_3$ , and  $\mathbf{x}_4$  are ready for the sparsity and incoherence calculations in compressed sensing described in Sec. 2. Correspondingly,  $\mathbf{y}_1$ ,  $\mathbf{y}_2$ ,  $\mathbf{y}_3$ , and  $\mathbf{y}_4$  can be obtained, and they are ready for the transmission over four independent channels. Here, the channels imply the packet-loss channel with the provided packet loss rate  $p_{e,i}$  in Fig. 2, with the subscript  $e$  and  $i$  denoting the error induced during transmission, and the channel number,  $1 \leq i \leq 4$ , respectively. We would expect that for transmitting the compressively sensed signals over multiple independent channels, reconstructed quality presents much better than those delivered over the single channel.

We describe the delivery of compressed sensing coefficients and propose our algorithm for error-controlled transmission as follows.

**3.1. Image compression with compressed sensing.** In this paper, we employ the test image `airport` with size of  $1024 \times 1024$  in Fig. 3. It serves as the input image  $\mathbf{x}$  in Fig. 1(a) or Fig. 1(c). We use large test images to show the performance capabilities of compressed sensing.

By following [9], for compressed sensing, we choose  $K_1 = 4,000$  coefficients in  $\Psi$  in Eq. (1), and  $K_2 = 80,000$  coefficients in  $\Phi$  in Eq. (2), from the  $1024 \times 1024 = 1,048,576$  pixels in the original image. With this setting, compression ratio of 262 times can be



FIGURE 3. Test image of airport, with size of  $1024 \times 1024$ .

reached. Figure 4 presents the reconstruction with compressed sensing coefficients after decompression, with the peak signal-to-noise ratio (PSNR) of 25.159 dB. Subjective and objective qualities in Fig. 4 serve as the baseline for the comparison with the following simulations for lossy transmission.

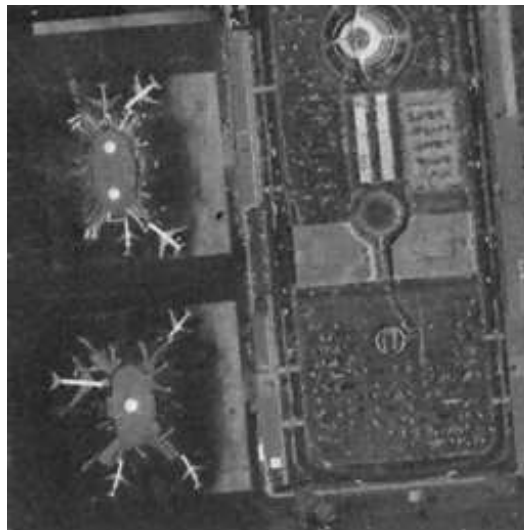


FIGURE 4. Compressed sensing of Fig. 3 with  $K_1 = 4,000$  and  $K_2 = 80,000$ . Resulting PSNR = 25.159 dB.

**3.2. Transmission of compressed sensing coefficients over multiple lossy channels.** With the extension to Fig. 1(d), in Fig. 2, compressed sensing coefficients from the four sub-sampled images, or  $\mathbf{y}_1$ ,  $\mathbf{y}_2$ ,  $\mathbf{y}_3$ , and  $\mathbf{y}_4$ , are ready for transmission over lossy channels, with similar concepts from [1, 16, 17]. The four channels are independent, and each channel corresponds to the lossy probability of  $p_{e,1}$ ,  $p_{e,2}$ ,  $p_{e,3}$ , and  $p_{e,4}$ , respectively. For example, if  $p_{e,1} = 0.25$ , it means that 25% of the compressed sensing coefficients may be lost during delivery. After transmission, coefficients of  $\tilde{\mathbf{y}}_1$ ,  $\tilde{\mathbf{y}}_2$ ,  $\tilde{\mathbf{y}}_3$ , and  $\tilde{\mathbf{y}}_4$  can be received at the decoder. Due to the possible loss during transmission,  $\tilde{\mathbf{y}}_i$  may not be identical to  $\mathbf{y}_i$ ,  $1 \leq i \leq 4$ .

### 3.3. Recovery of compressed sensing coefficients and reconstruction of image.

For transmission over lossy channels, every compressed sensing coefficient experiences the loss rate  $p_e$ , and it may be lost during transmission as depicted in Fig. 1(d). To alleviate the reconstruction quality, compressed sensing coefficients may be transmitted in parallel over multiple channels, and we choose four channels in this paper as depicted in Sec. 3.2 and in Fig. 2. Due to the high correlations between sub-sampled originals, compressed sensing coefficients tend to reach high correlations at the same transmission order. Once the coefficient is lost, it should be recovered from corresponding coefficients in other channels.

As we can see from the decoder part in Fig. 1(d), after the reception of compressed sensing coefficients  $\tilde{\mathbf{y}}$ , it follows the reverse operation to the encoding counterpart in Eq. (2):

$$\tilde{\mathbf{f}} = \Phi^{-1}\tilde{\mathbf{y}}. \quad (5)$$

Next,

$$\tilde{\mathbf{x}} = \Psi^{-1}\tilde{\mathbf{f}} = \Psi^{-1}\Phi^{-1}\tilde{\mathbf{y}}. \quad (6)$$

We may expect that for transmission over the single channel, due to channel error in  $\tilde{\mathbf{y}}$ , error propagation may cause the quality degradation in the reconstructed image of  $\tilde{\mathbf{x}}$ . By use of multiple channel transmission, reconstruction quality can be improved.

Due to the randomness in the packet-loss channels, it would not be as easy as reconstructing the scenario in Fig. 2. Still, we make comparisons with the coefficients of  $\tilde{\mathbf{y}}_1$ ,  $\tilde{\mathbf{y}}_2$ ,  $\tilde{\mathbf{y}}_3$ , and  $\tilde{\mathbf{y}}_4$  at the same position in the four channels. Suppose that we are going to examine the coefficient relationships at position  $k$ , or relationships of  $\tilde{y}_1[k]$ ,  $\tilde{y}_2[k]$ ,  $\tilde{y}_3[k]$ , and  $\tilde{y}_4[k]$  are ready to be checked. We first sort the magnitudes of the four received coefficients,  $|\tilde{y}_i[k]|$ ,  $1 \leq i \leq 4$ , in decreasing order. Without loss of generality, we assume that  $|\tilde{y}_1[k]| \geq |\tilde{y}_2[k]| \geq |\tilde{y}_3[k]| \geq |\tilde{y}_4[k]|$ . And there are several cases that are possible for the recovery of compressed coefficients. We omit the case that four coefficients are received correctly, or  $\tilde{y}_i[k] = y_i[k]$ ,  $1 \leq i \leq 4$ , because no reconstruction is necessary.

- Suppose one coefficient among the four is lost in this case. If the smallest magnitude, or  $|\tilde{y}_4[k]|$ , is smaller than some threshold  $\alpha$  (for example,  $\alpha = 5\%$ ) of the magnitude of the third coefficient, or  $|\tilde{y}_4[k]| < \alpha |\tilde{y}_3[k]|$ , the fourth coefficient is recovered by taking the median of the remaining three coefficients, or

$$\tilde{y}_4[k] = \text{median}(\tilde{y}_1[k], \tilde{y}_2[k], \tilde{y}_3[k]) = \tilde{y}_2[k]. \quad (7)$$

- Suppose two coefficients among the four are lost in this case. When  $|\tilde{y}_4[k]|$  and  $|\tilde{y}_3[k]|$  are both smaller than 5% of  $|\tilde{y}_2[k]|$ , we assume that  $\tilde{y}_4[k]$  and  $\tilde{y}_3[k]$  are lost. The lost coefficients are replaced by

$$\tilde{y}_4[k] = \text{median}(\tilde{y}_1[k], \tilde{y}_2[k]), \quad (8a)$$

$$\tilde{y}_3[k] = \text{median}(\tilde{y}_1[k], \tilde{y}_2[k]). \quad (8b)$$

- Suppose three coefficients among the four are lost in this case, or  $|\tilde{y}_4[k]|$ ,  $|\tilde{y}_3[k]|$ , and  $|\tilde{y}_2[k]|$  are all smaller than 5% of  $|\tilde{y}_1[k]|$ . All the lost coefficients are replaced by the first coefficient:

$$\tilde{y}_4[k] = \tilde{y}_1[k], \quad (9a)$$

$$\tilde{y}_3[k] = \tilde{y}_1[k], \quad (9b)$$

$$\tilde{y}_2[k] = \tilde{y}_1[k]. \quad (9c)$$

- Suppose all the four coefficients are lost in this case if the magnitude of the first coefficient lie below some small value around zero. No reconstruction is applicable.

After gathering all the recovered coefficients, reverse procedures to the encoding part should be performed as depicted in Fig. 2. The four sub-sampled images can first be recovered with Eq. (6), and by following Eqs. (4a) to (4d), reconstructed image from sub-sampled ones can be obtained.

With our algorithm, we expect to obtain enhanced performances with multiple-channel transmission in Fig. 2, than those with single-channel transmission, as depicted in Fig. 1(d).

**4. Simulation Results.** In our simulations, as we stated before, we choose the test image of *airport*, with the picture sizes of  $1024 \times 1024$ , for conducting simulations. As we noted in Sec. 3, in each sub-sampled image with size of  $512 \times 512$ , we set  $K_1 = 1,000$  compressed sensing coefficients, and  $K_2 = 20,000$  for noiselets for keeping the compression ratio.

Figure 5 demonstrates the resulting performance after experiencing 25% of loss rate over the single channel, causing the PSNR of 17.370 dB. Degradations can be easily observed by comparisons between Fig. 5 and Fig. 4. For simplicity, we split the original image into four sub-sampled images; each one experiences the compression with compressed sensing. For keeping the compression ratio, we choose  $K_1 = 1,000$  and  $K_2 = 20,000$  for each sub-sampled image with the size of  $512 \times 512$ , which corresponds to 25% of that in Fig. 4. Suppose that there are four channels for transmission in this paper. Then, coefficients corresponding to each sub-sampled images are transmitted over four independent channels in Fig. 2. Suppose Channel 1 is down, and Channels 2 to 4 are alive, which also results in the loss rate of 0.25. In Fig. 6, we demonstrate the scenarios described above. For making up the lost coefficients in Channel 1, we take the median value of corresponding coefficients in Channels 2, 3, and 4 to replace the lost coefficients in Channel 1. Recovered image is depicted in Fig. 7, with the PSNR = 23.467 dB. We can easily observe that the quality in Fig. 7 is much better than that in Fig. 5. Moreover, due to channel loss, even the reconstruction scheme is applied, the reconstructed quality in Fig. 7 is still a bit inferior to that in Fig. 4.



FIGURE 5. Compressively sensed image of Fig. 3 with  $K_1 = 4,000$  and  $K_2 = 80,000$ . Loss rate  $p_e = 0.25$ . Reconstructed PSNR = 17.370 dB.

Next, we consider transmitting compressed sensing images over independent lossy channels with  $p_{e,i} = 0.25$  for the ease of comparisons with Fig. 8. As we know, in Fig. 6, because only Channel 1 is down, we may imply that it is a deterministic channel, and hence the

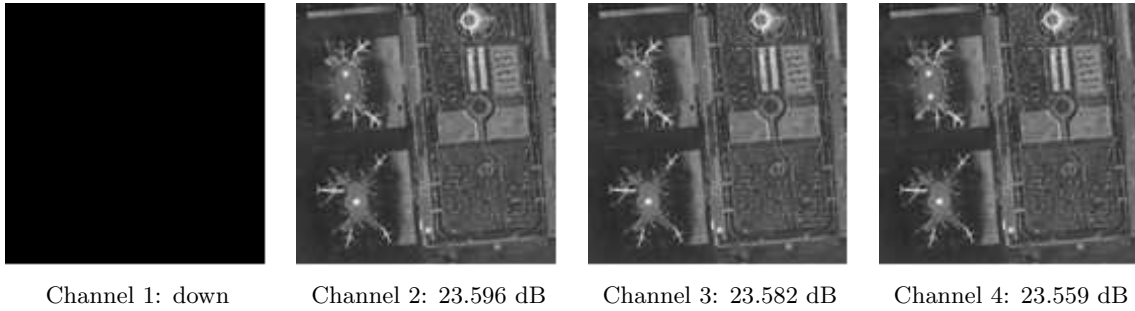


FIGURE 6. Transmission over multiple independent channels, with  $K_1 = 1,000$  and  $K_2 = 20,000$  for each channel. Suppose Channel 1 is down or  $p_{e,1} = 1.00$ , and Channels 2 to 4 are alive or  $p_{e,2} = p_{e,3} = p_{e,4} = 0.00$ . It leads to total loss rate of 0.25.

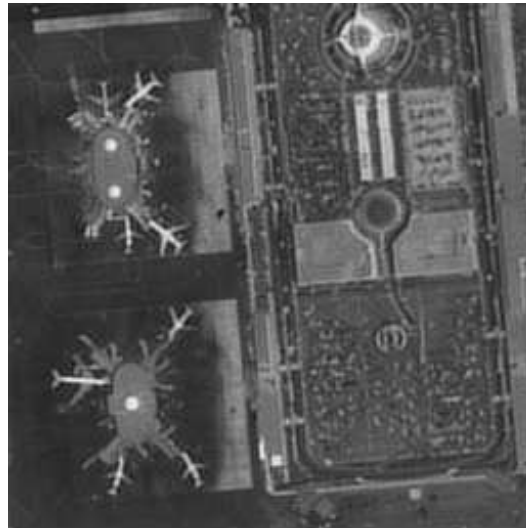


FIGURE 7. Recovery of coefficients in Channel 1 by taking the median from corresponding channels, and reconstruct the image from recovered Channel 1 coefficients and received coefficients from other channels. Reconstructed quality in PSNR = 23.467 dB.

reconstruction would be much easier than the random lossy channel. For the four independent channels in Fig. 2, we perform random loss with the probabilities of  $p_{e,i} = 0.25$ . Simulation results are depicted in Fig. 9. For the received image in Channel 1, because the large magnitude coefficients may be lost during transmission, severe degradation can be observed. For the reconstructed sub-sampled images from Channels 2 to 4, they result in similar qualities. With the reconstruction schemes described in Sec. 3.3, reconstructed image can be recovered by taking the median from the correctly received channels in Fig. 9.

We can also make comparisons between the results in Fig. 7 and Fig. 9. Reconstructed quality in Fig. 7 presents better than that in Fig. 9 even when the loss rates are 0.25 for the two cases. On the one hand, because we set the condition that Channel 1 is down in Fig. 6, which may imply the deterministic loss of Channel 1, reconstructed coefficients can all be correctly recovered. On the other hand, because we apply random loss for all coefficients among four channels, erroneous detection of lost coefficients may be expected, which leads

TABLE 1. Comparisons of difference loss rates between single- and multiple-channel transmission for test image `airport`. Reconstructed image quality is represented by peak signal-to-noise ratio in dB.

Loss rate	Single-channel reconstruction	Multiple-channel reconstruction
0.10	19.318 dB	22.423 dB
0.25	17.370 dB	22.044 dB
0.50	8.644 dB	20.195 dB

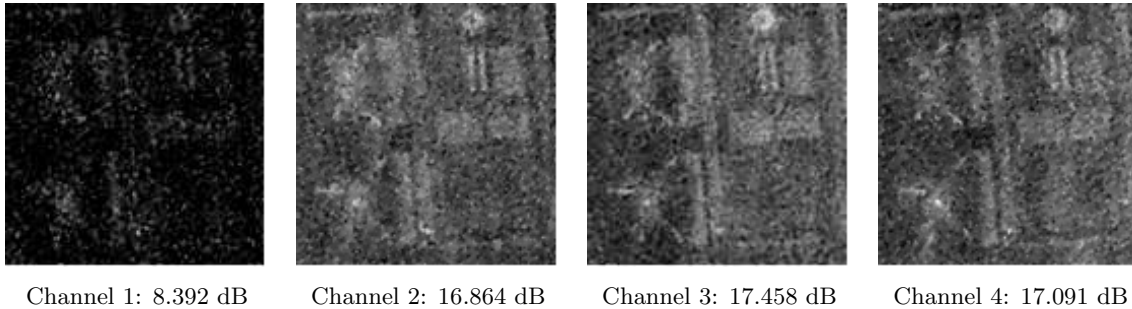


FIGURE 8. Transmission over multiple independent channels. Loss rate  $p_{e,i} = 0.25$  for each channel. Results in Channel 1 performs inferior because coefficients with large magnitudes are lost due to channel errors.



FIGURE 9. Recovery of coefficients by taking the median from correctly received channels. Reconstructed quality in PSNR = 22.044 dB.

to the degradation in image quality. From the results presented above, proposed algorithm point out the applicability for transmitting over lossy channels.

Finally, we make comparisons between the single-channel transmission and multiple-channel transmission over a variety of loss rates in Table 1. With the higher loss rates, reconstructed image quality becomes degraded. Besides, for the transmission over multiple channels with the recovery scheme provided, we can obtain better performances for the transmission with compressed sensing.

**5. Conclusions.** In this paper, we observed the vulnerability of compressively sensed information for transmission over lossy channels, and proposed our algorithm to transmit compressed information over multiple independent and lossy channels. Based on the experiences in the field of data compression, there is the need for protecting compressed coefficients, including compressively sensed ones, from channel errors for transmitting over lossy channels. There are high correlations between sub-sampled images in the original image. By use of transmitting compressively sensed coefficients from sub-sampled images, lost coefficients have the possibility to be recovered by use of taking the median from the correctly received coefficients from other channels. Simulation results have presented the enhanced performances with multiple channel transmission over single channel transmission of compressively sensed coefficients. We are going to look for other effective means to ensure the error-controlled transmission for compressed sensing of images.

**Acknowledgment.** The authors would like to thank Ministry of Science and Technology (Taiwan, R.O.C.) for supporting this paper under Grants No. MOST 103-2221-E-390-018, MOST 103-2221-E-032-052, and MOST 104-2221-E-390-012. The authors would also like to thank Mr. T. H. Wang for part of programming practices.

#### REFERENCES

- [1] S. S. Hemami, "Reconstruction-optimized lapped orthogonal transforms for robust image transmission," *IEEE Trans. Circuits and Systems for Video Tech.*, vol. 6, no. 2, pp. 168–181, Apr. 1996.
- [2] C. S. Shieh, H. C. Huang, and J. S. Pan, "The application of tabu search approach to energy allocation and index assignment for VQ-based binary phase shift keying," *Chinese Journal of Electronics*, vol. 11, no. 1, pp. 7–11, Jan. 2002.
- [3] E. J. Candès and M. B. Wakin, "An introduction to compressive sampling," *IEEE Signal Processing Magazine*, vol. 25, no. 2, pp. 21–30, Mar. 2008.
- [4] T. Arildsen and T. Larsen, "Compressed sensing with linear correlation between signal and measurement noise," *Signal Processing*, vol. 98, pp. 275–283, May 2014.
- [5] Compressed Sensing Resources, <http://dsp.rice.edu/cs>, Rice Univ. (accessed in Mar. 2015).
- [6] W. Jiang and J. Yang, "The rate-distortion optimized quantization algorithm in compressive sensing," *Optik — Int. J. for Light and Electron Optics*, vol. 125, no. 15, pp. 3980–3985, Aug. 2014.
- [7] M. L. Malloy and R. D. Nowak, "Near-optimal adaptive compressed sensing," *IEEE Trans. Information Theory*, vol. 60, no. 7, pp. 4001–4012, Jul. 2014.
- [8] T. Blumensath, "Compressed sensing with nonlinear observations and related nonlinear optimization problems," *IEEE Trans. Information Theory*, vol. 59, no. 6, pp. 3466–3474, Jun. 2013.
- [9] J. Romberg, "Imaging via compressive sampling," *IEEE Signal Processing Magazine*, vol. 25, no. 2, pp. 14–20, Mar. 2008.
- [10] C. Deng, W. Lin, B. S. Lee, and C. T. Lau, "Robust image coding based upon compressive sensing," *IEEE Trans. Multimedia*, vol. 14, no. 2, pp. 278–290, Apr. 2012.
- [11] H. C. Huang and F. C. Chang, "Robust image watermarking based on compressed sensing techniques," *J. of Information Hiding and Multimedia Signal Processing*, vol. 5, no. 2, pp. 275–285, Apr. 2014.
- [12] W. Li, J. S. Pan, L. J. Yan, C. S. Yang, and H. C. Huang, "Data hiding based on subsampling and compressive sensing," *Proc. Int'l Conf. on Robot, Vision and Signal Processing*, pp. 611–614, 2013.
- [13] L. Dai, Z. Wang, and Z. Yang, "Compressive sensing based time domain synchronous OFDM transmission for vehicular communications," *IEEE Journal on Selected Areas in Communications*, vol. 31, no. 9, pp. 460–469, Sep. 2013.
- [14] F. C. Chang and H. C. Huang, "Discussions on implementing iterative hard thresholding algorithm," *Proc. Int'l Conf. on Intelligent Information Hiding and Multimedia Signal Process.*, pp. 17–20, 2014.
- [15] F.C. Chang and H.C. Huang, "Comparison on different random basis generator of a single-pixel camera," *Proc. Int'l Conf. on Robot, Vision and Signal Processing*, pp. 1–4, 2013.
- [16] H. C. Huang and H. M. Hang, "Error control for low bit rate coding transmission," *Proc. IEEE Int'l Symp. Consumer Electronics*, pp. 165–168, 1997.
- [17] H. C. Huang and H. M. Hang, "Error resilient transmission with multiple description coding for image and video compression," *Proc. IEEE Int'l Symp. Consumer Electronics*, pp. 88–93, 2000.